

Cornell Interaction in the Two-body Pauli-Schrödinger-type Equation Framework: The Symplectic Quantum Mechanics Formalism

R.R. Luz*

*International Center for Physics, Instituto de Física, Universidade de Brasília, Brasília, DF, Brazil ,
Departamento de Física, Universidade Estadual do Maranhão, São Luís, MA, Brazil*

R.A.S. Paiva†

FCTE/Universidade de Brasília, Brasília, DF, Brazil

G.X.A. Petronilo‡

Universidade Federal do Pará, Salinópolis, PA, Brazil

A.E. Santana§, T.M. Rocha-Filho¶

International Center for Physics, Instituto de Física, Universidade de Brasília, Brasília, DF, Brazil

R.G.G. Amorim**

*International Center for Physics, Instituto de Física, Universidade de Brasília, Brasília, DF, Brazil ,
Canadian Quantum Research Center, Canada*

We investigate the quantum behavior of a quark-antiquark bound system under the influence of a magnetic field within the symplectic formulation of quantum mechanics. Employing a perturbative approach, we obtain the ground and first excited states of the system described by the Cornell potential, which incorporates both confining and non-confining interactions. After performing a Bohlin mapping in phase space, we solve the time-independent symplectic Pauli-Schrödinger-type equation and determine the corresponding Wigner function. Special attention is given to the observation of the confinement of the quark-antiquark, that is revealed in the phase space structure. Due to the presence of spin in the Hamiltonian, the results reveal that the magnetic field enhances the non-classicality of the Wigner function, signaling stronger quantum interference and a departure from classical behavior. The experimental mass spectra is used to estimate the intensity of the external field, leading to a value that is in order of the transient magnetic field measured in non-central heavy-ion collisions at RHIC and LHC.

I. INTRODUCTION

Particle physics aims to understand the fundamental laws of physics from basic structures, described by the standard model that addresses for instance fundamental interactions: the strong, weak and electromagnetic forces [1–6]. In more than half a century, particle accelerators allowed to access experimentally higher energies leading to the discovery of fundamental particles such as quarks [7–15]. These are particles confined in nature, with the gluons being the interacting field. This is the mechanism giving rise to hadrons [16, 17].

Different approaches have been developed to obtain predictions from the particle standard model, such as lattice calculations in quantum chromodynamics (QCD), effective field theory treatments, QCD sum rules and potential models [18]. Among the latter, a well known quark interaction is described by the Cornell (or funnel) potential. This model successfully takes into account the two crucial features of QCD, namely, the asymptotic freedom and the quark confinement [19, 20]. This is an important tool for examining the transition between the confined and deconfined phases of matter [21–24]. Beyond particle physics, the Cornell potential is of interest in other areas of physics such as nuclear physics, condensed matter and cosmology [25–33].

*Electronic address: renatoluzrgs@gmail.com

†Electronic address: rendisley@gmail.com

‡Electronic address: gustavopetronilo@gmail.com

§Electronic address: a.berti.santana@gmail.com

¶Electronic address: dimarti@unb.br

**Electronic address: ronniamorim@gmail.com

For a proper choice of units and covering a sector of QCD, the phenomenological Cornell potential is given by [34–37]

$$V(r) = -\frac{\alpha}{r} + \beta r, \quad (1)$$

where r is the inter-quark distance, $\alpha > 0$ is the quark-gluon coupling constant and β stands for the confinement constant [38–41]. In other words, the first (a Coulomb-like) term on the right side of Eq. (1) describes the one-gluon exchange between the quark-antiquark interaction; a dominant effect at short distances. The second (linear) term accounts for the quark confinement at large inter-quark separation [42–45]. In high energy, such a potential has been used for studying heavy quarkonia. This includes the calculation of masses of heavy quarkonium states by considering a quark-gluon plasma, as consisting of bound states of quarks and gluons [24, 46–49].

From a theoretical point of view, quarkonium systems such as $b\bar{b}$, $c\bar{c}$ and $\bar{b}c$ have been analyzed by using both relativistic and non-relativistic wave equations, which are solved by employing different approaches [50]. This is the case, for instance, of considering the following aspects: an extra dimension, as an extension of the Cornell potential [51]; an inclusion of a harmonic oscillator term for the Dirac equation [52]; a Lie algebraic method of quasi-exactly solvable systems [54]; the asymptotic iteration method [19, 55, 56]; the mass spectrum of bottomonium has been also analyzed by using Gaussian wave functions [62]; bound states of the finite temperature-dependent Schrödinger equation for an extended Cornell potential were also calculated [58], such that the mass spectra of heavy quarkonia and the B_c meson at both zero and nonzero temperatures were derived; and the method supersymmetric expansion algorithm-(SEA) has been utilized to obtain analytical solutions, leading to relativistic corrections. Hence, it was possible to extract general qualitative and quantitative predictions for the bottomonium and charmonium spectrum which nicely agree with experimental data [64].

The Schrödinger equation with the Cornell potential in an Euclidian non-commutative space has been analyzed [53]. In this framework, it was obtained analytical solutions and spectral properties for the deformed Schrödinger, Dirac and Klein-Gordon equations. These developments utilize the Bopp shift method and perturbation theory in the phase-space Wigner function [59–61]. Along the same direction, solutions of the symplectic Schrödinger equation provided, as an instance, characteristics of the confinement-deconfinement due to the structure of the quantum phase-space representation [18]. More recently a generalized Cornell potential for heavy quark interaction was considered in the context of the Nikiforov-Uvarov method, with fractional derivatives in the framework of the symplectic quantum mechanics [63].

As an Euclidian potential, usually the Schrödinger equation for a boson is used to analyze the spectrum and the evolution of the quark system. Nevertheless, since the quark is a fermion the (non-relativistic) Pauli-Schrödinger equation should be of interest. Indeed, this aspect was explored to analyze the Casimir effect for the confined quark-antiquark system, near the region of $V(r) = 0$ [65], in Eq. (1). In this case, the symplectic representation of quantum mechanics was used, providing improvements in the results on confinement due to the presence of spin [66].

The symplectic representation of Schrödinger equation is intimately associated with the Wigner function formalism, which has been widely used in the literature, as in particle systems [67]. The Wigner function can be reconstructed from optical homodyne tomography [68, 69] or directly sampled point-by-point by using photon counting and displacement techniques [70–72]. It is a powerful tool for determining the statistical characteristics of quantum states such as non-classicality and aspects of chaoticity. These properties are crucial not only in the fields of quantum computing and quantum information but also play a significant role in particle physics [63, 67, 73–75].

In the present work, we study the quantum-mechanical problem of a quarkonium moving in the Cornell potential, by using the symplectic quantum mechanics approach including the spin effect. Our main goals and procedure are the following. (a) We use symmetry to derive the symplectic representation of the Pauli-Schrödinger equation. (b) Aspects of the confinement are investigated considering experimental results. (c) The experimental spectrum is considered in order to estimate the intensity of the external field. (d) The emergency of non-classicality in the quarkonium states are analyzed as a function of the external field. In order to solve the symplectic Pauli-Schrödinger equation, the Levi-Civita map and the standard perturbation theory up to first and second order are used. This leads to the Wigner function for the quark-antiquark bound state due to a Cornell potential and a magnetic field.

The work is organized as follows. In Section II, in order to fix the notation, we discuss basic aspects of the symplectic Schrödinger equation, and the relation between the Schrödinger phase-space wave function (a quasi-amplitude of probability) and Wigner function (a quasi-distribution of probability). Section III presents the quark-antiquark description using the Symplectic Pauli-Schrödinger equation, with the Cornell potential in the presence of an external magnetic field. Section IV brings the discussions for the results. Some final concluding remarks are presented in Section V.

II. NON-RELATIVISTIC SYMPLECTIC QUANTUM MECHANICS

In this section, some aspects of the non-relativistic symplectic formulation of quantum mechanics for boson are presented [66]. Consider the set Γ of the points with coordinates (q, p) , $q, p \in \mathbb{E}$, where \mathbb{E} is the Euclidian space. When equipped with the symplectic 2-form $w = dq \wedge dp$, Γ is denominated phase space. A Hilbert space in Γ , say $\mathcal{H}(\Gamma)$, is formed by the set of C^∞ functions $\phi(q, p)$ with the property

$$\int dq dp \phi^\dagger(q, p) \phi(q, p) < \infty.$$

A basis in $\mathcal{H}(\Gamma)$ is given by $|q, p\rangle$, with dual $\langle q, p|$, and satisfying the property

$$\int dq dp |q, p\rangle \langle q, p| = 1.$$

For a vector $|\phi\rangle \in \mathcal{H}(\Gamma)$ and its dual $\langle\phi|$, the following relations are fulfilled: $\phi(q, p) = \langle q, p|\phi\rangle$, and $\phi^\dagger(q, p) = \langle\phi|q, p|$. Unitary mappings $U(\alpha)$ in $\mathcal{H}(\Gamma)$ are defined by $U(\alpha) = \exp(-i\alpha \hat{A})$, where the generator of symmetry \hat{A} is given by

$$\begin{aligned} \hat{A} &= A(q, p) \star = A(q, p) \exp \left[\frac{i\hbar}{2} \left(\frac{\overleftarrow{\partial}}{\partial q} \frac{\overrightarrow{\partial}}{\partial p} - \frac{\overleftarrow{\partial}}{\partial p} \frac{\overrightarrow{\partial}}{\partial q} \right) \right] \\ &= A(\hat{Q}, \hat{P}), \end{aligned} \quad (2)$$

with

$$\hat{P} = p \star = p - \frac{i\hbar}{2} \partial_q, \quad (3)$$

$$\hat{Q} = q \star = q + \frac{i\hbar}{2} \partial_p. \quad (4)$$

Here, the following notation for derivatives is used, i.e., $\partial_q \equiv \partial/\partial q$, $\partial_p \equiv \partial/\partial p$. The arrows in Eq. (2) mean that the respective operator acts on a function at its left (right) according to the orientation of the arrow \leftarrow (\rightarrow). The star (or Weyl) product, \star , is defined by

$$\star \equiv \exp \left[\frac{i\hbar}{2} \left(\frac{\overleftarrow{\partial}}{\partial q} \frac{\overrightarrow{\partial}}{\partial p} - \frac{\overleftarrow{\partial}}{\partial p} \frac{\overrightarrow{\partial}}{\partial q} \right) \right].$$

From now on we will set units such that $\hbar = 1$, the speed of light is $c = 1$ and the electron charge $e = 1$, unless necessary for clarifying the units.

In the symplectic framework for quantum mechanics the Heisenberg commutation relation is written as $[\hat{Q}_j, \hat{P}_k] = i\delta_{jk}$, with $j, k = 1, 2, 3$. Then the operators $\hat{Q} = (\hat{Q}_1, \hat{Q}_2, \hat{Q}_3)$ and $\hat{P} = (\hat{P}_1, \hat{P}_2, \hat{P}_3)$ stand for the observables position and momentum, respectively. Considering the Galilei symmetries, the following operators are defined:

$$\hat{K}_i \equiv m\hat{Q}_i - t\hat{P}_i, \quad \hat{L}_i \equiv \epsilon_{ijk}\hat{Q}_j\hat{P}_k, \quad \hat{H} \equiv \frac{\hat{P}^2}{2m}. \quad i = 1, 2, 3.$$

Here m stands for the mass of a particle. The operators \hat{P} , \hat{K} , \hat{L} and \hat{H} are then the generators of Galilei symmetries, standing for spatial translation (linear momentum), Galilean boosts, rotation (the angular momentum), and time translation (the Hamiltonian), respectively.

The time-translation generator \hat{H} provides the time evolution of a wave function in phase space $\psi(q, p, t_0)$ from a initial time t_0 to a time t by writing

$$\psi(q, p, t) = e^{\hat{H}(t-t_0)}\psi(q, p, t_0),$$

which is the formal solution of the Schrödinger equation in phase space, i.e.,

$$\partial_t \psi(q, p; t) = \hat{H}(q, p)\psi(q, p; t), \quad (5)$$

also called the symplectic Schrödinger equation [81]. The physical interpretation of this formalism is given by the relation of the phase-space wave function $\psi(q, p, t)$ with the Wigner function, $f_W(q, p, t)$ [81–83, 86, 87], that is

$$f_W(q, p, t) = \psi(q, p, t) \star \psi^\dagger(q, p, t).$$

Since $f_W(q, p, t)$ is a quasi-distribution of probability, $\psi(q, p, t)$ is interpreted as a quasi-amplitude of probability [18, 87–89]. For our proposals here, it is important to write the eigenvalue version of Eq. (5), i.e.

$$\hat{H}(q, p)\psi(q, p; t) = H(q, p) \star \psi(q, p) = E\psi(q, p) \quad (6)$$

All the results reviewed above are directly generalized for N -dimensions. It is important also to note that Eq. (5) describes particle with spin zero. In the next section this approach is generalized to consider particles with spin 1/2.

III. QUARK-ANTIQUARK BOUND STATES

Here the bound states of the quark-antiquark system from the symplectic formulation are derived. Initially, the classical non-relativistic Hamiltonian for a bound state of a “charged” and massive quark and its antiquark system is written as

$$H = \frac{1}{2m} (\mathbf{P}'^2 - \boldsymbol{\sigma} \cdot \mathbf{B}) + V(\mathbf{r}), \quad (7)$$

where $\boldsymbol{\sigma} = (\sigma_x, \sigma_y, \sigma_z)$ are the Pauli matrices, $\mathbf{P}' = \mathbf{P} - (e/c)\mathbf{A}$ is the kinetic momentum for a minimal coupling, \mathbf{P} the canonical momentum, m the reduced mass of the quark-antiquark system, \mathbf{A} the magnetic vector potential and $V(\mathbf{r})$ the interaction potential.

For a spatially uniform magnetic field in the z direction $\mathbf{B} = B\hat{z}$, the vector potential is written as $\mathbf{A} = (-\frac{B}{2}y, \frac{B}{2}x, 0)$. Substituting this potential in Eq. (7), the kinetic term takes the form

$$\mathbf{P}'^2 = \frac{1}{2m} (\mathbf{P} - e\mathbf{A})^2 = \frac{1}{2m} \left[\left(P_x + \frac{eBy}{2} \right)^2 + \left(P_y - \frac{eBx}{2} \right)^2 \right]. \quad (8)$$

This leads to

$$\frac{1}{2m} (\mathbf{P} - e\mathbf{A})^2 = \frac{P_x^2 + P_y^2}{2m} + \frac{e^2 B^2 (x^2 + y^2)}{8m} - \frac{eB}{2m} (xP_y - yP_x). \quad (9)$$

The last term is identified as the orbital magnetic coupling, proportional to the angular momentum $L_z = xP_y - yP_x$. The Hamiltonian is then written as

$$H = \left[\frac{P_x^2 + P_y^2}{2m} + \frac{B^2 e^2 (x^2 + y^2)}{8m} - \frac{eBL_z}{2m} - e\hbar\sigma_z B \right] + eV(r). \quad (10)$$

Considering the spin term, it is assumed that the orbital angular momentum, L_z , term is very small. That is, the spin term is predominant over the orbital movement. And as such, the Hamiltonian is rewritten as into that of a two-dimensional harmonic oscillator in the presence of the Cornell potential and a magnetic field [18, 87, 89, 95], that is,

$$H = \left[\frac{P_x^2 + P_y^2}{2m} + \frac{B^2 e^2 (x^2 + y^2)}{8m} - e\hbar\sigma_z B \right] - \frac{\alpha}{r} + \beta r, \quad (11)$$

where Eq. (1) is used for $V(r)$. In order to address the Coulomb-like term in the Cornell potential, the Bohlin mapping (or Levi-Civita transformation) is considered now. The Bohlin mapping is introduced here by

$$x = q_1^2 - q_2^2, \quad (12)$$

$$y = 2q_1 q_2, \quad (13)$$

$$P_x = \frac{p_1 q_1 + p_2 q_2}{2(q_1^2 + q_2^2)}, \quad (14)$$

$$P_y = \frac{p_2 q_1 - p_1 q_2}{2(q_1^2 + q_2^2)}. \quad (15)$$

Substituting Eqs. (12)-(15) in Eq. (11) and using $r = \sqrt{x^2 + y^2} = q_1^2 + q_2^2$ and $\sigma_z = \pm 1$, it leads to

$$H = \left[\frac{p_1^2 + p_2^2}{8m(q_1^2 + q_2^2)} + \frac{B^2(q_1^2 + q_2^2)^2}{8m} - \frac{\pm B}{2m} \right] - \frac{\alpha}{(q_1^2 + q_2^2)} + \beta(q_1^2 + q_2^2). \quad (16)$$

Considering the hypersurface in phase space given by $H = E$, where E is a constant, it leads to

$$\left(\frac{p_1^2 + p_2^2}{2m} \right) - \frac{\pm B}{2m} (q_1^2 + q_2^2) - 4E(q_1^2 + q_2^2) + \frac{B^2(q_1^2 + q_2^2)^3}{2m} - 4\beta(q_1^2 + q_2^2)^2 - 4\alpha = 0. \quad (17)$$

It is important to emphasize that the Bohlin mapping is a canonical transformation [89, 95]. In this sense, the physical content of the Hamiltonian in Eq. (17) is the same as in its quantum version. In order to obtain the symplectic quantization, we have to multiply the right side of Eq. (17) by $\star\Psi(q, p)$, leading to

$$\left[\left(\frac{p_1^2 + p_2^2}{2m} \right) - \frac{\pm B}{2m} (q_1^2 + q_2^2) - 4E(q_1^2 + q_2^2) + \frac{B^2(q_1^2 + q_2^2)^3}{2m} - 4\beta(q_1^2 + q_2^2)^2 - 4\alpha \right] \star \Psi = 0, \quad (18)$$

Note that this equation is obtained from the classical Hamiltonian through of the star product, according to Eq. (6).

Looking for a perturbative approach, Eq. (18) is rewritten as

$$[\hat{H}_0 + \hat{H}_1] \Psi(q_1, p_1, q_2, p_2) = 4\alpha\Psi(q_1, p_1, q_2, p_2), \quad (19)$$

where \hat{H}_0 and \hat{H}_1 are the unperturbed and perturbed Hamiltonians, respectively, given by

$$\hat{H}_0 = \frac{1}{2m}(p_1^2 + p_2^2) \star - \left(\frac{\pm B}{2m} - 4E \right) (q_1^2 + q_2^2) \star, \quad (20)$$

$$\hat{H}_1 = \frac{B^2(q_1^2 + q_2^2)^3}{2m} \star - 4\beta(q_1^2 + q_2^2)^2 \star. \quad (21)$$

The field $\Psi(q, p)$ is the two-component Pauli-Schrödinger spinor, written as

$$\Psi = \begin{pmatrix} \psi_1 \\ \psi_2 \end{pmatrix}. \quad (22)$$

In Eq. (20), the frequency, ω , of the two harmonic oscillators is given by

$$\omega^2 = - \left(\frac{\pm B}{m^2} - \frac{8E}{m} \right). \quad (23)$$

It is important to notice that Eq. (19) looks like an auto-value equation, although α is a constant due to the Cornell potential. Despite this fact, in order to find solutions of Eq. (19), it is possible to consider α as an non-fixed constant. At the end of the calculations the original value of α will be recovered. In the following, perturbation procedures will be carried out, initially with the zero order.

A. Zero order solution

Using the fact that the Hamiltonian \hat{H}_0 is that of a two-dimensional isotropic harmonic oscillator, we solve the zero order equation $\hat{H}_0\Psi^{(0)} = \alpha_{n_1, n_2}^{(0)}\Psi^{(0)}$, leading to

$$\Psi(q_1, p_1, q_2, p_2) = \phi_{n_1}(q_1, p_1)\phi_{n_2}(q_2, p_2), \quad (24)$$

where $\phi_n(q, p)$ is the stationary state of the one-dimensional harmonic oscillator with quantum number n .

We now define the star creation and annihilation operators:

$$\begin{aligned}\hat{a} &= \left(\sqrt{\frac{\omega}{2}} q_1 \star + i \sqrt{\frac{1}{2\omega}} p_1 \star \right), \\ \hat{a}^\dagger &= \left(\sqrt{\frac{\omega}{2}} q_1 \star - i \sqrt{\frac{1}{2\omega}} p_1 \star \right), \\ \hat{b} &= \left(\sqrt{\frac{\omega}{2}} q_2 \star + i \sqrt{\frac{1}{2\omega}} p_2 \star \right), \\ \hat{b}^\dagger &= \left(\sqrt{\frac{\omega}{2}} q_2 \star - i \sqrt{\frac{1}{2\omega}} p_2 \star \right),\end{aligned}\tag{25}$$

These operators satisfy the following relations:

$$\begin{aligned}[\hat{a}, \hat{a}^\dagger] &= [\hat{b}, \hat{b}^\dagger] = 1, \\ \hat{a} \phi_{n_1}(q_1, p_1) &= \sqrt{n_1} \phi_{n_1-1}(q_1, p_1), \\ \hat{a}^\dagger \phi_{n_1}(q_1, p_1) &= \sqrt{n_1+1} \phi_{n_1+1}(q_1, p_1), \\ \hat{b} \phi_{n_2}(q_2, p_2) &= \sqrt{n_2} \phi_{n_2-1}(q_2, p_2), \\ \hat{b}^\dagger \phi_{n_2}(q_2, p_2) &= \sqrt{n_2+1} \phi_{n_2+1}(q_2, p_2).\end{aligned}\tag{26}$$

In addition, it is useful to note that

$$\begin{aligned}q_k \star &= \frac{1}{\sqrt{2\omega}} (\hat{a} + \hat{a}^\dagger), \\ p_k \star &= -i \sqrt{\frac{\omega}{2}} (\hat{a} - \hat{a}^\dagger),\end{aligned}\tag{27}$$

$k = 1, 2$, and

$$\hat{a}^\dagger \hat{a} \psi_{n_1, n_2}^{(0)} = n_1 \psi_{n_1, n_2}^{(0)}, \quad \hat{b}^\dagger \hat{b} \psi_{n_1, n_2}^{(0)} = n_2 \psi_{n_1, n_2}^{(0)}.\tag{28}$$

The unperturbed and perturbed Hamiltonian are, respectively, rewritten as

$$\begin{aligned}\hat{H}_0 &= \omega (\hat{a}^\dagger \hat{a} + \hat{b}^\dagger \hat{b} + 1), \\ \hat{H}_1 &= \frac{B^2}{16m\omega^3} [(\hat{a} + \hat{a}^\dagger)^2 + (\hat{b} + \hat{b}^\dagger)^2]^3 - \frac{\beta}{\omega^2} [(a + a^\dagger)^2 + (b + b^\dagger)^2]^2.\end{aligned}\tag{29}$$

The eigenvalues of the undisturbed Hamiltonian in the state ϕ_{n_1, n_2} are then

$$\alpha_{n_1, n_2}^{(0)} = \frac{1}{4}(n_1 + n_2 + 1)\omega.\tag{30}$$

As addressed before, in this zero order, the parameter $\alpha_{n_1, n_2}^{(0)}$ has to be restricted to the original value as α in the Cornell potential. Therefore, by using the definitions of ω and Eq. (30), we obtain the zero order energy spectrum

$$E_{n_1, n_2}^{(0)} = \frac{2m\alpha^2}{(n_1 + n_2 + 1)^2} \pm \frac{B}{8m}.\tag{31}$$

It is important to observe that the limit $B \rightarrow 0$ these result agrees with previous zero-field results [80, 88].

The quasi-amplitudes of probability functions are obtained by noticing that

$$\hat{a} \phi_0 = 0, \quad \hat{b} \phi_0 = 0.\tag{32}$$

Using Eq. (25), it leads to

$$\left(\sqrt{\frac{\omega}{2}} q_1 \star + i \sqrt{\frac{1}{2\omega}} p_1 \star \right) \phi_0 = 0,\tag{33}$$

such that

$$\Psi_{0,0}^{(0)}(q_1, p_1, q_2, p_2) = N e^{-(\omega q_1^2 + p_1^2)} L_{n_1}(\omega q_1^2 + p_1^2) e^{-(\omega q_2^2 + p_2^2)} L_{n_2}(\omega q_2^2 + p_2^2), \quad (34)$$

where L_n are Laguerre polynomials of order n and N is a normalization constant. The excited states are derived by using the raising operators \hat{a}^\dagger and \hat{b}^\dagger as is usual.

B. First order correction

The first-order correction to the eigen-functions in usual perturbation theory is given by

$$\Psi_{n_1, n_2}^{(1)}(q_1, p_1, q_2, p_2) = \Psi_{n_1, n_2}^{(0)}(q_1, p_1, q_2, p_2) + \sum_{m_1 \neq n_1; m_2 \neq n_2} \frac{\mathcal{I}}{\alpha_{n_1, n_2}^{(0)} - \alpha_{m_1, m_2}^{(0)}}, \quad (35)$$

where

$$\mathcal{I} = \langle \Psi_{m_1, m_2}^{*(0)}(q_1, p_1, q_2, p_2) | \hat{H}^{(1)} | \Psi_{n_1, n_2}^{(0)}(q_1, p_1, q_2, p_2) \rangle. \quad (36)$$

Using the orthogonality relations

$$\langle \phi_n^*(q_1, p_1) | \phi_m(q_1, p_1) \rangle = \delta_{n,m}, \quad (37)$$

$$\langle \Gamma_n^*(q_2, p_2) | \Gamma_m(q_2, p_2) \rangle = \delta_{n,m}, \quad (38)$$

the meson ground state is then

$$\begin{aligned} \Psi_{0,0}^{(1)} = \Psi_{0,0}^{(0)} - \frac{1}{\omega} \left[\left(\frac{9\sqrt{2}B^2}{4m\omega^3} - \frac{4\sqrt{2}\beta}{\omega^2} \right) \Psi_{2,0}^{(0)} + \left(\frac{9B^2}{8m\omega^3} - \frac{\beta}{\omega^2} \right) \Psi_{2,2}^{(0)} + \left(\frac{9\sqrt{6}B^2}{16m\omega^3} - \frac{\sqrt{6}\beta}{2\omega^2} \right) \Psi_{4,0}^{(0)} \right. \\ \left. + \frac{\sqrt{3}B^2}{8m\omega^3} \Psi_{4,2}^{(0)} + \frac{\sqrt{5}B^2}{8m\omega^3} \Psi_{6,0}^{(0)} \right]. \end{aligned} \quad (39)$$

The eigenfunction for the first excited state is given by

$$\begin{aligned} \Psi_{1,0}^{(1)} = \Psi_{1,0}^{(0)} - \frac{1}{\omega} \left[\sqrt{2} \left(\frac{9B^2}{2m\omega^3} - \frac{6\beta}{\omega^2} \right) \Psi_{1,2}^{(0)} + \sqrt{6} \left(\frac{3B^2}{4m\omega^3} - \frac{\beta}{2\omega^2} \right) \Psi_{1,4}^{(0)} \right. \\ \left. + \sqrt{6} \left(\frac{9B^2}{2m\omega^3} - \frac{6\beta}{\omega^2} \right) \Psi_{3,0}^{(0)} + \sqrt{3} \left(\frac{3B^2}{2m\omega^3} - \frac{\beta}{\omega^2} \right) \Psi_{3,2}^{(0)} + \frac{3B^2}{8m\omega^3} \Psi_{3,4}^{(0)} \right. \\ \left. + \frac{\sqrt{5}B^2}{8m\omega^3} \Psi_{1,6}^{(0)} + \sqrt{30} \left(\frac{3B^2}{4m\omega^3} - \frac{\beta}{2\omega^2} \right) \Psi_{5,0}^{(0)} + \frac{\sqrt{15}B^2}{8m\omega^3} \Psi_{5,2}^{(0)} + \frac{\sqrt{35}B^2}{8m\omega^3} \Psi_{7,0}^{(0)} \right], \end{aligned} \quad (40)$$

and

$$\begin{aligned} \Psi_{0,1}^{(1)} = \Psi_{0,1}^{(0)} - \frac{1}{\omega} \left[\sqrt{2} \left(\frac{9B^2}{2m\omega^3} - \frac{6\beta}{\omega^2} \right) \Psi_{2,1}^{(0)} + \sqrt{6} \left(\frac{9B^2}{2m\omega^3} - \frac{6\beta}{\omega^2} \right) \Psi_{0,3}^{(0)} \right. \\ \left. + \sqrt{3} \left(\frac{3B^2}{2m\omega^3} - \frac{\beta}{\omega^2} \right) \Psi_{2,3}^{(0)} + \sqrt{6} \left(\frac{3B^2}{4m\omega^3} - \frac{\beta}{2\omega^2} \right) \Psi_{4,1}^{(0)} + \sqrt{30} \left(\frac{3B^2}{4m\omega^3} - \frac{\beta}{2\omega^2} \right) \Psi_{0,5}^{(0)} \right. \\ \left. + \frac{3B^2}{8m\omega^3} \Psi_{4,3}^{(0)} + \frac{\sqrt{5}B^2}{8m\omega^3} \Psi_{6,1}^{(0)} + \frac{\sqrt{15}B^2}{8m\omega^3} \Psi_{2,5}^{(0)} + \frac{\sqrt{35}B^2}{8m\omega^3} \Psi_{0,7}^{(0)} \right]. \end{aligned} \quad (41)$$

The Wigner function for quark-antiquark bound states is then obtained from these eigen-states by using the \star product as

$$f_W(q_1, p_1, q_2, p_2) = \Psi_{n_1, n_2}^{(1)}(q_1, p_1, q_2, p_2) \star \Psi_{n_1, n_2}^{\dagger(1)}(q_1, p_1, q_2, p_2). \quad (42)$$

Since the eigenfunction is real, then the Wigner function is the eigenfunction itself. For ground state the Wigner function is given by

$$f_W(q_1, p_1, q_2, p_2) = \Psi_{0,0}^{(1)}(q_1, p_1, q_2, p_2) \star \Psi^{\dagger(1)}(q_1, p_1, q_2, p_2) \propto \Psi_{0,0}^{(1)}(q_1, p_1, q_2, p_2) \quad (43)$$

The first-order correction for the eigenvalues is obtained from

$$\Delta\alpha_{n_1, n_2}^{(1)} = \int \Psi_{n_1, n_2}^{(0)} \widehat{H}_1 \Psi_{n_1, n_2}^{\dagger(0)} dq_1 dp_1 dq_2 dp_2, \quad (44)$$

Substituting \widehat{H}_1 , we have

$$\Delta\alpha_{n_1, n_2}^{(1)} = \int \Psi_{n_1, n_2}^{(0)} \left\{ \frac{B^2}{16m\omega^3} \left[(\hat{a} + \hat{a}^\dagger)^2 + (\hat{b} + \hat{b}^\dagger)^2 \right]^3 - \frac{\beta}{\omega^2} \left[(a + a^\dagger)^2 + (b + b^\dagger)^2 \right]^2 \right\} \Psi_{n_1, n_2}^{\dagger(0)} dq_1 dp_1 dq_2 dp_2,$$

which yields

$$\Delta\alpha_{n_1, n_2}^{(1)} = \frac{B^2}{16m\omega^3} \Delta' - \frac{\beta}{\omega^2} \Delta'', \quad (45)$$

where

$$\Delta' = \left[20(n_1^3 + n_2^3) + 18(n_1^2 n_2 + n_1 n_2^2) + 42(n_1^2 + n_2^2) + 36n_1 n_2 + 46(n_1 + n_2) + 48 \right] \quad (46)$$

and

$$\Delta'' = \left[6n_1^2 + 6n_2^2 + 8n_1 n_2 + 10n_1 + 10n_2 + 8 \right]. \quad (47)$$

In this way, we obtain the result for the first-order corrected eigenvalue

$$\alpha_{n_1, n_2}^{(1)} = \frac{1}{4}(n_1 + n_2 + 1)\omega + \frac{B^2}{16m\omega^3} \Delta' - \frac{\beta}{\omega^2} \Delta''. \quad (48)$$

For the ground state ($n_1 = 0, n_2 = 0$), the second-order perturbation eigenvalue correction is given by

$$4\alpha_{0,0}^{(2)} \approx \omega + \left(\frac{3B^2}{m\omega^3} - \frac{8\beta}{\omega^2} \right) + \left(-\frac{249}{4} \frac{B^4}{m^2\omega^7} + 180 \frac{B^2\beta}{m\omega^6} - 144 \frac{\beta^2}{\omega^5} \right). \quad (49)$$

Using the Eq. (31) and Eq. (45), the energy spectrum up to first order is calculated as

$$E_{n_1, n_2}^{(1)} = \frac{m}{8} \frac{\left(4\alpha - \frac{B^2}{16m\omega^3} \Delta' + 4 \frac{\beta}{\omega^2} \Delta'' \right)^2}{(n_1 + n_2 + 1)^2} \pm \frac{B}{8m}. \quad (50)$$

This result gives the energy eigenvalues for a quarkonium particle described by the Cornell potential in the presence of an external field. Specific cases are analyzed in the next section.

IV. STATIONARY-STATE WIGNER FUNCTIONS

In this section we analyze the Wigner function of the stationary states describing the quark-antiquark system, up to the first order approximation, considering the $c\bar{c}$, $b\bar{b}$, mesons obtained by using the symplectic quantum mechanics approach. In the lowest bound state $c\bar{c}$ has a mass of roughly 3.5 times greater than the proton mass [1, 18, 20, 63]. We obtained here the ground state with the respective quasi-amplitude probability. For the numerical analysis, the following parameter values are used [42]: the confinement parameter $\beta = 0.191 \text{ GeV}^2$, charm quark mass $m_c = 1.3205 \text{ GeV}$, bottom quark mass $m_b = 1.3205 \text{ GeV}$, the reduced mass $m_{c\bar{c}} = 0.6602 \text{ GeV}$, $m_{b\bar{b}} = 2.374 \text{ GeV}$, frequency values are $\omega = 2.71 \text{ GeV}$ for $c\bar{c}$ and $\omega = 2.26 \text{ GeV}$ for $b\bar{b}$, see Appendix (A). In addition, we also take the parameters $q_1 = q$ and $p_1 = p$ with $(q_2 = p_2 = 0)$ fixed in the graphical representation. It is important to emphasize that the unit of q^2 is GeV^{-1} ; i.e., q^2 stands for the physical inter-quark distance.

The left graphics of Fig. (1) and Fig. (2), display the first-order corrected behavior of the Wigner function $f_W(q_1, p_1; q_2 = 0, p_2 = 0)$ for the ground state ($n_1 = 0, n_2 = 0$) of the mesons $c\bar{c}$ and $b\bar{b}$, with fixed momentum

$p = 0$ GeV and the right graphics for momentum variations $p = 2.3$ GeV (red), 2.5 GeV (green), and 2.9 GeV (blue) with no external magnetic field ($B = 0$).

In the graphics on the right of Fig. (1) and Fig. (2) we observe that for momentum $p = 0$ GeV, and for $B = 0$ GeV 2 , the Wigner function exhibits the graphical behavior in accordance with a previous result [18]. That is, $p = 0$ represents a limiting condition for the existence of the $c\bar{c}$, $b\bar{b}$ mesons system that goes from $q^2 = 0$ to $q^2 \approx 4$ GeV $^{-1}$. This means that the system is confined in that region, a result that is in accordance with experimental results [18]. In Fig. (1) (right graph) and Fig. (2) (right graph), it is observed that by varying the momentum $p = 2.3$ GeV (red line), $p = 2.5$ GeV (green line), and $p = 2.9$ GeV (blue line), with $B = 0$ GeV 2 , the Wigner function shifts to the left and the peaks of the curve decrease within the region $q^2 = 0$ to $q^2 \approx 4$ GeV $^{-1}$. For larger values of momentum the Wigner function disappears, that is, the meson systems does not exist. Then, there is an upper limit for the existence of the $c\bar{c}$, $b\bar{b}$ mesons which is given by the curves of the Wigner function as shown in Fig. (1) and Fig. (2). It is within the symplectic quantum mechanics representation that the confinement mechanism is revealed through of the Wigner function. The symplectic formulation allows this confining behavior to emerge naturally through the geometry of phase space. Our findings is in line with previous results [18, 45].

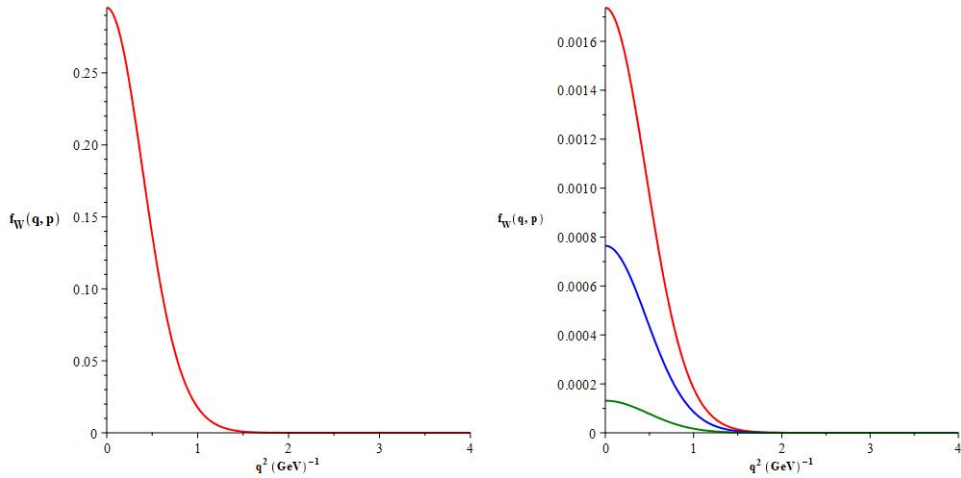


FIG. 1: The left graph, first-order corrected Wigner function for the ground state ($n_1 = 0$, $n_2 = 0$) of the $c\bar{c}$ meson, with momentum $p = 0$ GeV and no magnetic field ($B = 0$ GeV 2), plotted as a function of the interquark distance q^2 in the region $0 \leq q^2 \lesssim 4$ GeV $^{-1}$. The right graph, the Wigner function is presented for the same state with momenta $p = 2.3$ GeV (red), 2.5 GeV (green), and 2.9 GeV (blue), also for $B = 0$ GeV 2 .

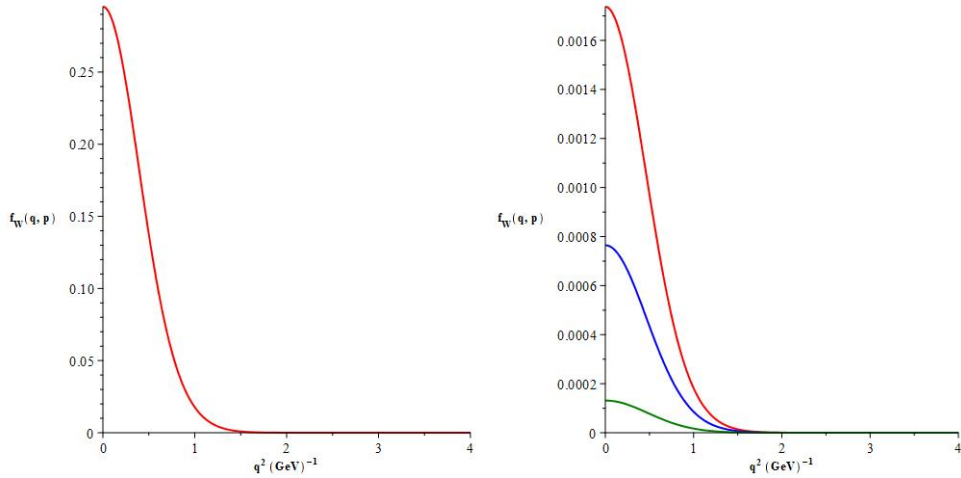


FIG. 2: The left graph, Wigner function with first-order correction for the state ($n_1 = 0$, $n_2 = 0$) (ground state) of the $b\bar{b}$ meson with $p = 0$ GeV and $B = 0$ GeV 2 . The right graph, the Wigner function is plotted for the same state with momenta $p = 2.3$ GeV (red), 2.5 GeV (green), and 2.9 GeV (blue), also for $B = 0$ GeV 2 .

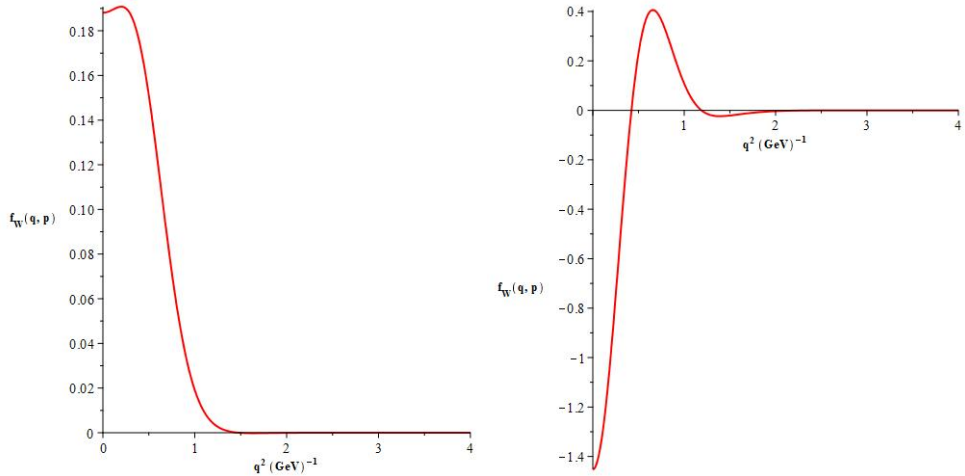


FIG. 3: The left graph, Wigner function with first-order correction for the state ($n_1 = 0, n_2 = 0$) (ground state) of the $c\bar{c}$ meson with $p = 0$ GeV and $B = 1.5$ GeV 2 . The right graph is plot for the Wigner function considering the same state but with $B = 4.5$ GeV 2 and for $p = 0$ GeV.

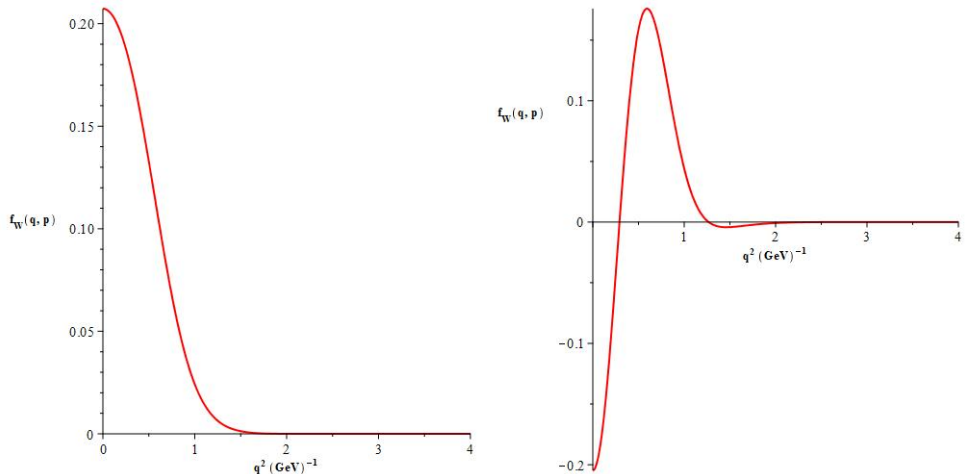


FIG. 4: The left graph, Wigner function with first-order correction for the state ($n_1 = 0, n_2 = 0$) (ground state) of the $b\bar{b}$ meson with $p = 0$ GeV and $B = 1.5$ GeV 2 . The right graph, the Wigner function is presented for the same state with $B = 4.5$ GeV 2 and for $p = 0$ GeV.

Figures (3) and (4) illustrate the first-order corrected Wigner function for the same eigen-state ($n_1 = 0, n_2 = 0$), but considering the non-zero magnetic field. In Fig. 3, for $B = 1.5$ GeV 2 , $B = 4.5$ GeV 2 , the behavior of the Wigner function is described for the $c\bar{c}$ meson. In Fig. 4, for $B = 1.5$ GeV 2 , $B = 4.5$ GeV 2 , shows the behavior of the Wigner function for the $b\bar{b}$ meson. Note that for different values of the magnetic field, B , the statistical nature of the Wigner functions changes due to the emergence of negative regions. This negativity is an indicator non-classicality of the system. It is worth noting that field values are arbitrary, and are taken here just to show the effect of B on the statistical characteristic of the state. In the sequence, the mass spectrum is analyzed and an experimental value for B is considered.

Tables I presents the ground-state mass spectrum of the $c\bar{c}$, $b\bar{b}$ mesons computed using the first-order energy correction, in comparison with experimental data. Table II provides various theoretical predictions available in the literature which are compared to the experimental results.

These mass spectra is given by the following equation [20]

$$M = m_q + m_{\bar{q}} + E + V_0. \quad (51)$$

Substituting Eq. (23) in Eq. (51), it leads to

$$M = m_q + m_{\bar{q}} + \frac{m}{8} \omega^2 + \frac{(\pm B)}{8m}. \quad (52)$$

where m_q , $m_{\bar{q}}$ are the masses of the quark-antiquark, respectively, and m is the reduced mass. Table I show the mass spectrum corresponding to the ground state of the $c\bar{c}$ and $b\bar{b}$ mesons with regard to the experimental data.

TABLE I: Fundamental energy level and mass spectrum of the $c\bar{c}$, $b\bar{b}$ mesons (in GeV), calculated by using the present model and compared with experimental data and various theoretical works. Parameters used: $\alpha = 0.472$, $\beta = 0.191$ GeV 2 , $V_0 = -1.55$ GeV for $(b\bar{b})$, $V_0 = 0$ GeV for $(c\bar{c})$, $m_c = 1.3205$ GeV, $m_{c\bar{c}} = 0.6602$ GeV, $m_b = 4.7485$ GeV, $m_{b\bar{b}} = 2.374$ GeV [42]. In both of the cases we obtained a value of the external field B , that fits the experimental value of M .

Meson	State	ω	$-B \rightarrow M$	M	$+B \rightarrow M$	M	Exp. [94]
$c\bar{c}$	$n_1 = n_2 = 0$	2.24	0.203	3.019	0.203	3.097	3.097
$b\bar{b}$	$n_1 = n_2 = 0$	2.26	0.194	9.460	0.194	9.460	9.460

TABLE II: Fundamental energy level and mass spectrum of the $c\bar{c}$, $b\bar{b}$ mesons (in GeV), calculated by using the different model and different parameter choices [42].

Meson	$M \rightarrow$	Ref. [11]	Ref. [19]	Ref. [78]	Ref. [45]	Ref. [63]	Ref. [55]	Ref. [79]	Ref. [42]	Exp. [94]
$c\bar{c}$		3.074	3.078	3.098	3.1003	3.0966	3.0954	3.095	3.098	3.097
$b\bar{b}$		9.460	9.506	9.681	9.4818	9.4564	9.74473	9.460	9.460	9.460

In Table I, for the $c\bar{c}$ meson ground state at $\omega = 2.24$ GeV, the mass spectrum equation yields two field magnitudes that reproduce the experimental mass when the negative sign associated with the $\pm B/(8m)$ term is chosen. Specifically, the model gives $B = 0.203$ GeV 2 for $M = 3.097$ GeV and $B = -0.203$ GeV 2 for $M = 3.019$ GeV. When the field value is taken to be positive ($+B$), the mass spectrum value of the meson $c\bar{c}$ are consistent with the experimental value 3.097 GeV [94]. For $B = -0.203$ GeV 2 , the predicted masses, yields $M = 3.019$ GeV regarding the meson $c\bar{c}$.

In Table I, for $b\bar{b}$ meson ground state, and $\omega = 2.26$ GeV, the spectrum exhibits the two field values in $\pm B/(8m)$ term in Eq. (52). Our model gives $B = 0.194$ GeV 2 for $M = 9.460$ GeV and $B = -0.194$ GeV 2 for $M = 9.460$ GeV. In the case of meson $b\bar{b}$, both field values ($+B$) and ($-B$) are consistent with experimental value $M = 9.460$ GeV [94].

Table II benchmarks the ground-state masses against several theoretical determinations [11, 19, 42, 45, 55, 63, 78, 79] and experiment [94]. For $c\bar{c}$ meson, the values are near the experimental mass 3.097 GeV, spanning approximately 3.074 – 3.1003 GeV, while for $b\bar{b}$ meson they span roughly 9.4564–9.74473 GeV, referent to the experimental value 9.460 GeV. Note that this comparison indicates that the ground-state predictions are of the same order and precision as widely used approaches in the literature, and that agreement with experiment can be obtained (notably through the appropriate choice of the sign and field magnitude in Table I).

Although the perturbative expressions derived here are valid for arbitrary (n_1, n_2) , in this work we present explicit numerical results mainly for the ground-state $1S$ heavy quarkonia, since the ground state provides the most accurate measured experimental data. Regarding the quantitative validation of model here presented, the conversion of the values derived here for the parameter B , given in GeV 2 , to SI units reveals effective fields of the order of 10^{15} T. Although this magnitude may seem excessive for static laboratory magnets, it is fully consistent with estimates for transient magnetic fields in non-central heavy-ion collisions, which can reach 10^{14} T at RHIC and up to approximately 10^{15} T at LHC [96]. Notably, these fields are of the same order of magnitude as the energy scales characteristic of gluon interactions and the QCD vacuum, playing a crucial role in the dynamics of strong interactions [96].

V. FINAL CONCLUDING REMARKS

In the present work, the symplectic quantum mechanics has been applied to obtain the ground and excited states of a quark-antiquark system, within a perturbative framework. The quarks are interacting through the Cornell potential in an external magnetic field.

First, a symplectic representation of the Pauli-Schrödinger-type equation has been derived by using a phase space representation of Galilei group. This equation is then solved by following a Bohlin mapping associated with a

perturbative method. This theoretical procedure leads to the Wigner function for the quark-antiquark bound state. Aspects of the confinement are then investigated, providing consistent results with experimental data. These results are inherently manifest due to the phase-space geometry. The effect of the external field on the statistical nature the quarkonium state is analyzed. In fact, aspects of no-classicality are revealed in the dependence with different values of the external field.

The experimental spectrum is considered in order to estimate the intensity of the external field, B . The results for the mass spectrum are, in particular, compared with other models in the literature. Another result is that the model introduced here provides a value for B in the order of 10^{15} T. This value, which is consistent with the mass spectrum, is in the order of the intensity of transient magnetic fields taking place in non-central heavy-ion collisions. These transient fields reaches 10^{14} T at RHIC and up to 10^{15} T at LHC [96].

Finally, regarding the perturbative approach, the main part of the analysis has been carried out up to first order approximation, although the energy spectrum has also been derived up to second order. A detailed analysis of higher orders in the perturbative method is an aspect that demands significantly more computational effort; and as such, these results will be presented elsewhere.

Acknowledgments

This work is partially supported by the Brazilian funding agency CNPq (Conselho Nacional de Desenvolvimento Científico e Tecnológico-Brazil), grant numberis 312857/2021-7 (TMRF).

Appendix A

Here, we have shown the explicit calculations of frequency and magnetic field values that fit the experimental mass spectrum for the mesons $c\bar{c}$ and $b\bar{b}$. To obtain the frequency and magnetic field values B , we use the already defined parameters and the given equations.

For the ground state ($n_1 = 0, n_2 = 0$), the second-order perturbation eigenvalue correction is given by

$$4\alpha_{0,0}^{(2)} \approx \omega + \left(\frac{3B^2}{m\omega^3} - \frac{8\beta}{\omega^2} \right) + \left(-\frac{249}{4} \frac{B^4}{m^2\omega^7} + 180 \frac{B^2\beta}{m\omega^6} - 144 \frac{\beta^2}{\omega^5} \right). \quad (\text{A1})$$

Using the Eq. (23) and isolating E we have

$$E = \frac{m}{8} \omega^2 + \frac{(\pm B)}{8m}. \quad (\text{A2})$$

The equation above is substituted into Eq. (52) leading to

$$M = m_q + m_{\bar{q}} + \frac{m}{8} \omega^2 + \frac{(\pm B)}{8m}. \quad (\text{A3})$$

Considering the parameters α , β , m_c , $m_{c\bar{c}}$, the experimental value M for meson $c\bar{c}$ listed in table I and substituting in Eq. (A3) and (A1) we have

$$\begin{cases} 1.888 = \omega + \left(\frac{3B^2}{m\omega^3} - \frac{8\beta}{\omega^2} \right) + \left(-\frac{249}{4} \frac{B^4}{m^2\omega^7} + 180 \frac{B^2\beta}{m\omega^6} - 144 \frac{\beta^2}{\omega^5} \right), \\ 0.456 = 0.082525 \omega^2 + (\pm 0.1893366 B). \end{cases} \quad (\text{A4})$$

By solving the equation system we obtain the field value $(\pm B)$ and ω for $c\bar{c}$ system,

$$\omega \approx 2.24, \quad B \approx 0.203 \text{ GeV}^2. \quad (\text{A5})$$

An analogous procedure can be carried out for the meson $b\bar{b}$.

[1] S. Godfrey and N. Isgur, Phys. Rev. D **32**, 189 (1985).

[2] G.S. Bali, Phys. Rep. **343**, 1 (2001).

[3] H. Grosse and A.J. Martin, *Particle Physics and the Schrödinger Equation*, (Cambridge University Press, Cambridge, 1997).

[4] L.P. Fulcher, Z. Chen, and K.C. Yeong, Phys. Rev. D **47**, 4122 (1993).

[5] W. Lucha, and F.F. Schöberl, *Phenomenological aspects of nonrelativistic potential models*, (Oesterreichische Akademie der Wissenschaften, 1989).

[6] S.N. Gupta, S.F. Radford, and W.W. Repko, Phys. Rev. D, **26**, 3305 (1982).

[7] R. Mann, *An introduction to particle physics and the standard model*, (CRC press, New York, 2009).

[8] W. Marciano, and H. Pagels, Phys. Rep. **36**, 137 (1978).

[9] M. Abu-Shady, Indonesian J. Combinatorics **7**, 94 (2023).

[10] M. Abu-Shady, and E.M. Khokha, Int. J. Mod. Phys. A. **36**, 2150195 (2021).

[11] M. Abu-shady and H. M. Fath-Allah, arXiv:2309.14310 [hep-ph], (2023)

[12] S. Gasiorowicz, *Elementary particle physics* (Wiley, New York, 1966).

[13] D. Griffiths, *Introduction to elementary particles* (John Wiley & Sons, New York, 2008).

[14] I.J.R. Aitchison, and A.J.G. Hey, *Gauge Theories in Particle Physics: A Practical Introduction: From Relativistic Quantum Mechanics to QED* (IOP Publishing, Bristol, 2012).

[15] M. Thomson, *Modern Particle Physics* (Cambridge University Press, Cambridge, 2013).

[16] E. Omugbe, E.P. Inyang, I.J. Njoku, C. Martínez-Flores, A. Jahanshir, I.B. Okon, E.S. Eyube, R. Horchani, and C.A. Onate, Nucl. Phys. A **1034**, 122653, (2023).

[17] N. Brambillaa, and A. Vairo, Proc. 13th Ann. Hamp. Univ. Grad. Stud., HUGS **98**, 151 (1998).

[18] R.R. Luz, C.S. Costa, G.X.A. Petronilo, A.E. Santana, R.G.G. Amorim, and R.A.S. Paiva, Adv. High Energy Phys. **2022**, 10 (2022).

[19] R. Kumar and F. Chand, Commun. Theor. Phys. **59**, 528 (2013).

[20] H. Mansour and A. Gamal, Adv. High Energy Phys. **2018**, 7 (2018).

[21] R.C.L. Bruni, E.F. Capossoli, and H. Boschi-Filho, Adv. High Energy Phys. **2019**, 6 (2019).

[22] E.V.B. Leite, H. Belich, and R.L.L. Vitória, Adv. High Energy Phys. **2019**, (2019).

[23] M. Abu-shady, H.M. Fath-Allah, Sci Rep **15**, 1875 (2025).

[24] S. Koothottil, J.P. Prasanth, and V.M. Bannur, In Proceedings of the DAE Symp. on Nucl. Phys. **62**, 912 (2017).

[25] F. Tajik, Z. Sharifi, M. Eshghi, M. Hamzavi, M. Bigdeli, and S.M. Ikhdair, Phys. A. **535**, 122497 (2019).

[26] W.N. Cottingham, and D.A. Greenwood, *An introduction to the standard model of particle physics* (Cambridge university press, Cambridge, 2007).

[27] H. Hassanabadi, E. Maghsoodi, and S. Zarrinkamar, Ann. Phys. (Berlin) **525**, 944 (2013).

[28] M. Abu-Shady, S.Y. Ezz-Alarab, Few-Body Syst. **62**, 13 (2021).

[29] R.J. Lombard, J. Mareš and C. Volpe, J. Phys. G: Nucl. Part. Phys. **34**, 1879 (2007).

[30] L. Jenkovszky, Y.A. Kurochkin, N.D. Shaikovskaya, and V.O. Soloviev, Universe **10**, 76 (2024).

[31] V. Kumar, S.B. Bhardwaj, R.M. Singh, and F. Chand, Mol. Phys. **120**, (2022).

[32] M. Hosseinpour, H. Hassanabadi, and M. de Montigny, Int. J. Geom. Meth. Mod. Phys. **15**, 1850165 (2018).

[33] E. Spallucci, and A. Smailagic, Phys. Lett. B **846**, 138257 (2023).

[34] A. Maireche, Int. J. Phys., Chem. Astron. **88**, 1 (2022).

[35] E. Eichten et al., Phys. Rev. Lett. **34**, 369 (1975).

[36] E. Eichten et al., Phys. Rev. D **17**, 3090 (1978).

[37] B. Bukor, and J. Tekel, Eur. Phys. J. Plus, **138**, 499 (2023).

[38] M. Abu-Shady, J. Egypt. Math. Soc. **25**, 86 (2017).

[39] H. Ciftci, and H.F. Kisoglu, Pramana J. Phys. **57**, 458 (2018).

[40] M. Hamzavi, and A.A. Rajabi, Ann. Phys. (NY) **334**, 316 (2013).

[41] H.S. Chung, J. Lee, and D. Kang, J. Korean Phys. Soc. **52**, 1151 (2008).

[42] H. Mutuk, Adv. High Energy Phys. **2019**, 9 (2019).

[43] N. Ferkous and A. Bounames, Commun. Theor. Phys. **59**, 679 (2013).

[44] S.M. Ikhdair, Adv. High Energy Phys. **2013**, 10 (2013).

[45] R.R. Luz, M. Abu-Shady, G.X.A. Petronilo, A.E. Santana, and R.G.G. Amorim, Adv. High Energy Phys. **2023**, 7 (2023).

[46] A.I. Ahmadov, C. Aydin, and O. Uzun, J. Phys.: Conf. Ser. **1194**, 012001 (2019).

[47] T.S. Ramazanov, Zh. A. Moldabekov, and M.T. Gabdullin, Phys. Plasmas **23**, 042703 (2016).

[48] I. Aref'eva, K. Rannu, and P. Slepov, EPJ Web Conf. **222**, 03023 (2019).

[49] M. Abu-Shady, Int. J. Mod. Phys. A **34**, 1950201 (2019).

[50] A. Vega, J. Flores, Pramana - J. Phys. **87**, 73 (2016).

[51] J. Lahkar, Few-Body Sys. **64**, 22 (2023).

[52] M. Abu-Shady, B. J. Mod. Phys. **1**, 16 (2015).

[53] A. Al-Jamel, J. Theor. and Appl. Phys. **5**, 21 (2011).

[54] H. Panahi, S. Zarrinkamar, and M. Baradaran, Eur. Phys. J. Plus **131**, 35 (2016).

[55] E.M. Khokha, M. Abu-Shady, and T.A. Abdel-Karim, Int. J. Theor. Appl. Phys. **2**, 86 (2016).

[56] R.L. Hall and N. Saad, Open Phys. **13**, 83 (2015).

[57] G. Nowaskie, Int. J. Theor. Phys. **62**, 186 (2023).

[58] A.I. Ahmadov, K.H. Abasova, and M.S. Orucova, Adv. High Energy Phys.,**2021**, 1861946 (2021).

[59] A. Maireche, J. Nano- Electron. Phys. **8**, 01020 (2016). [https://doi.org/10.21272/jnep.8\(1\).01020](https://doi.org/10.21272/jnep.8(1).01020)

[60] A. Maireche. & D. Imane, *J. Nano- Electron. Phys.* **8**, 03025 (2016). [10.21272/jnep.8\(3\).03025](https://doi.org/10.21272/jnep.8(3).03025).

[61] A. Maireche, *Jordan J. Phys.* **14**, 1 (2021). <https://doi.org/10.47011/14.1.6>.

[62] V. Kher, R. Chaturvedi, N. Devlani, and A.K. Rai, *Eur. Phys. J. Plus* **137**, 357 (2022).

[63] M. Abu-Shady, R.R. Luz, G.X.A. Petronilo, A.E. Santana, and R.G.G. Amorim, *Int. J. Mod. Phys. A* **39**, 2450011 (2024).

[64] M. Napsuciale, S. Rodríguez, and A. E. Villanueva-Gutiérrez, *Phys. Rev. D* **111**, 116022 (2025).

[65] G.X.A. Petronilo, R.G.G. Amorim, S.C. Ulhoa, A.F. Santos, A.E. Santana, and F.C. Khanna, *Int. J. Mod. Phys. A* **36**, 2150121 (2021).

[66] A.E. Santana, F.C. Khanna, A.F. Santos, R.G.G. Amorim, S.C. Ulhoa, J. D. M. Vianna, *Symplectic Quantum Field Theory* 1.ed. (Cambridge Scholars Publishing, Newcastle upon Tyne, England. 2024).

[67] S. Jana, V.K. Ojha, and T. Maji, *Nucl. Phys. A* **1053**, 122958 (2025).

[68] D.T. Smithey, M. Beck, M.G. Raymer, and A. Faridani, *Phys. Rev. Lett.* **70**, 1244 (1993).

[69] G. Breitenbach, S. Schiller, and J. Mlynek, *Nature* **387**, 471 (1997).

[70] D.K. Ferry, and M. Nedjalkov, *The Wigner function in science and technology*, (IoP Publishing, 2018).

[71] K. Banaszek, and K. Wódkiewicz, *Phys. Rev. Lett.* **76**, 4344 (1996).

[72] M.S. Najafabadi, L.L. Sánchez-Soto, K. Huang, J. Laurat, H. Le Jeannic, and G. Leuchs, *Phil. Trans. R. Soc. A* **382**, 20230337 (2024).

[73] C. Lorce and B. Pasquini, *Phys. Rev. D* **84**, 014015 (2011).

[74] R. Radhakrishnan and V.K. Ojha, *Mod. Phys. Lett. A* **37**, 2250236 (2022).

[75] J. Weinbub and D. Ferry, *Appl. Phys. Rev.* **5**, 4 (2018).

[76] A. Al-Jamel, *Int. J. Mod. Phys. A* **34**, 1950054 (2019).

[77] A. Jahanshir, et al., *Open Phys.* **22**, 20240004 (2024).

[78] E. Omugbe, E. S. William, O. E. Osafire, I. B. Okon, E. P. Inyang and A. Jaha, *Few-Body Syst.* **63**, 6 (2022).

[79] M. Abu-Shady, T. A. Abdel-Karim and Sh. Y. Ezz-Alarab, *J. Egypt. Math. Soc.* **27**, 14 (2019).

[80] X.L. Yang, S.H. Guo, F.T. Chan, K.W. Wong, and W.Y. Ching, *Phys. Rev. A* **43**, 1186 (1991).

[81] M.D. Oliveira, M.C.B. Fernandes, F.C. Khanna, A.E. Santana, and J.D.M. Vianna, *Ann. Phys.* **312**, 492 (2004).

[82] H. Dessano, R.A.S. Paiva, R.G.G. Amorim, S.C. Ulhoa, and A.E. Santana, *Braz. J. Phys.* **49**, 715 (2019).

[83] R.G.G. Amorim, R.A.S. Paiva, *Advan. Theor. and Comput. Phys.* **1**, (2018).

[84] C. Mena, and L.F. Palhares, arXiv preprint arXiv:1804.09564, (2018).

[85] V. Mateu, P.G. Ortega, D.R. Entem, and F. Fernández, *Eur. Phys. J. C* **79**, 1 (2019).

[86] A.X. Martins, R.A.S. Paiva, G.X.A. Petronilo, R.R. Luz, R.G.G. Amorim, S.C. Ulhoa, and T.M.R. Filho, *Adv. High Energy Phys.* **2020**, 6 (2020).

[87] R.A.S. Paiva, R.G.G. Amorim, S.C. Ulhoa, A.E. Santana, and F.C. Khanna, *Adv. High Energy Phys.* **2020**, 9 (2020).

[88] P. Campos, M.G.R. Martins, M.C.B. Fernandes, and J.D.M. Vianna, *Ann. Phys. (NY)* **390**, 60 (2018).

[89] P. Campos, M.G.R. Martins, and J.D.M. Vianna, *Phys. Lett. A* **381**, 1129 (2017).

[90] W. Lucha, F.F. Schöberl, and D. Gromes, *Phys. Rep.* **200**, 127 (1991).

[91] H. Mutuk, *Adv. High Energy Phys.* **2018**, 5961031 (2018).

[92] N.R. Soni, B.R. Joshi, R.P. Shah, H.R. Chauhan, and J.N. Pandya, *Eur. Phys. J. C* **78**, 1 (2018).

[93] M.N. Sergeenko, *Adv. High Energy Phys.* **2013**, 325431 (2013).

[94] R.L. Workman et al. (Particle Data Group), *Prog. Theor. Exp. Phys.* 2022, 083C01 (2022).

[95] A. Celletti, *Basics of regularization theory.*, In: *Chaotic Worlds: From Order to Disorder in Gravitational N-Body Dynamical Systems*. Lect. Notes Phys., **227**. (Springer, Dordrecht. 2006) https://doi.org/10.1007/978-1-4020-4706-0_7

[96] M. D'Elia, F. Negro, *Phys. Rev. D* **83**, 114028 (2011).